International Journal of Environmental Sciences
ISSN: 2229-7359
Vol. 11 No. 22s, 2025
https://theaspd.com/index.php

Design, Optimization, And Evaluation of Terbinafine-Loaded Nanogel for Enhanced Transungual Delivery and Antifungal Efficacy Against Onychomycosis

Rushikesh Ganeshrao Pawade[1], Souvik Sur[2], Neeraj Kumar Tripathi[3], Rajat Garg[4], Trishna Mani Nath[5], Lathika R[6], Divya Rajan[7], Garima Verma[8]

[1]Professor, Datta Meghe Ayurvedic Medical College Hospital and Research Centre Nagpur 441110 India
[2]Assistant Professor, Teerthanker Mahaveer University, Moradabad, Uttar Pradesh 244001 India
[3]Assistant Professor, P.B.P.G. College (PRSU Prayagraj), Pratapgarh, Uttar Pradesh 230002 India
[4]Assistant Professor, Department of Pharmacy, Institute of Biomedical Research and Education, Mangalayatan University, Beswan, Aligarh, Uttar Pradesh 202146 India
[5]Assistant Professor, University of Science and Technology Meghalaya, Techno City, Kiling Road, Baridua, 9th Mile, Ri-Bhoi, Meghalaya 793101 India
[6]Associate Professor, Ahalia School of Optometry and Research Centre, Ahalia Foundation Eye Hospital, Ahalia Campus, Kozhipara (PO), Palakkad, Kerala 678557 India
[7]Assistant Professor, Indira Gandhi Institute of Pharmaceutical Sciences, Perumbavoor, Ernakulam, Kerala 683549 India
[8]Professor, Faculty of Pharmacy, Swami Vivekanand Subharti University, Meerut, Delhi -Haridwar bypass Road, Subhartipuram, Meerut, Uttar Pradesh 250005 India
Corresponding Author: Garima Verma
Designation and Affiliation: Professor, Faculty of Pharmacy, Swami Vivekanand Subharti University, Meerut, Delhi -Haridwar bypass Road, Subhartipuram, Meerut, Uttar Pradesh 250005 India
Email id: garima.srivastava2111@gmail.com

Abstract

The present study focuses on the ***design, optimization, and evaluation of terbinafine-loaded nanogel*** *aimed at enhancing transungual drug delivery and antifungal efficacy against onychomycosis. Pre-formulation studies confirmed terbinafine's higher solubility in propylene glycol and compatibility with selected excipients through FTIR and DSC analyses. The nanogel was prepared using an emulsification–ionic gelation method and optimized via a Quality by Design (QbD) approach. Characterization studies revealed a mean particle size of ~ 118 nm, narrow PDI (0.21), and a zeta potential of −28 mV, indicating good stability. TEM imaging confirmed spherical nanoparticles in the range of 36–43 nm. The optimized formulation demonstrated shear-thinning rheology, pH within the physiological range (5.6), high drug content uniformity (~ 98%), and entrapment efficiency (>90%). In vitro drug release studies using dialysis and Franz diffusion cells showed sustained release (>90% at 24 h), following Higuchi kinetics with anomalous transport mechanism. Nail penetration studies confirmed a ~ 3-fold increase in drug flux and ~ 3-fold higher drug retention in nail plates compared to pure terbinafine suspension. Antifungal activity assessments revealed significantly lower MIC and MFC values for the nanogel (0.25–0.5 μg/ml) compared to suspension (1–2 μg/ml), along with larger inhibition zones (32 mm vs. 21 mm against* T. rubrum*). Time-kill assays further confirmed rapid fungicidal action, achieving complete kill within 24 h for nanogel, whereas suspension required up to 48 h. These findings demonstrate that terbinafine-loaded nanogel provides* ***enhanced solubility, sustained release, improved transungual penetration, and superior antifungal efficacy*** *compared to conventional formulations. This nanogel system holds promise as a potential topical therapeutic approach for effective and patient-compliant management of onychomycosis.*

Keywords: *Terbinafine, Nanogel, Transungual Delivery, Onychomycosis, Antifungal Efficacy*

1. INTRODUCTION

Onychomycosis is a common and persistent fungal infection that affects both fingernails and toenails, leading to nail discoloration, thickening, brittleness, and eventual dystrophy. Beyond cosmetic concerns, it significantly impacts patients' quality of life by causing discomfort, social stigma, and functional limitations in daily activities [1]. The prevalence of onychomycosis increases with age and is especially high among individuals with comorbid conditions such as diabetes mellitus, peripheral vascular disease, and immunosuppression [2]. Complications associated with untreated or recurrent infection include secondary bacterial infections and ulceration, which can be severe in vulnerable populations like diabetics,

further highlighting the need for effective therapeutic interventions [3]. The etiological spectrum of onychomycosis includes dermatophytes, non-dermatophyte molds, and yeasts [4]. Dermatophytes, particularly Trichophyton rubrum, are the most frequent causative agents, exploiting their keratinolytic activity to invade the nail bed and plate [5]. Yeasts such as Candida albicans commonly affect fingernails, particularly in individuals with prolonged water exposure or compromised immunity, while non-dermatophyte molds like Aspergillus and Scopulariopsis species contribute to infections in select cases [6]. The ability of these organisms to persist within the dense keratin structure of nails and form resistant biofilms makes eradication challenging [7]. The current therapeutic landscape includes both oral and topical antifungal agents [8]. Oral drugs such as terbinafine, itraconazole, and fluconazole provide systemic efficacy but are often limited by hepatotoxicity, drug–drug interactions, and the need for prolonged administration [9]. On the other hand, topical treatments such as ciclopirox and amorolfine lacquers are safer but face significant barriers due to poor nail penetration, slow onset of visible improvement, and the requirement for long-term application [10]. High recurrence rates and poor patient compliance with lengthy regimens further compromise treatment success [11]. Among oral agents, terbinafine is widely considered the gold standard due to its fungicidal mechanism [12]. Belonging to the allylamine class, terbinafine inhibits squalene epoxidase, an essential enzyme in the ergosterol biosynthesis pathway, leading to disruption of fungal cell membrane integrity and accumulation of toxic squalene [13]. While terbinafine demonstrates potent efficacy against dermatophytes, its therapeutic potential is hampered by poor nail penetration and systemic side effects associated with long-term use [14]. These limitations justify the need for innovative strategies to enhance terbinafine's local delivery to the site of infection. Nanotechnology has emerged as a promising approach in antifungal therapy, particularly through the development of nanogels [15]. Nanogels are three-dimensional, cross-linked polymeric systems that can encapsulate drugs at the nanoscale, improving their solubility, stability, and sustained release properties. When applied to nail drug delivery, nanogels offer distinct advantages such as enhanced penetration through the keratinized nail plate, prolonged drug retention, controlled release, reduced dosing frequency, and minimized systemic absorption [16]. These attributes make them ideal candidates for overcoming the barriers associated with conventional onychomycosis therapies. Despite the therapeutic advances of terbinafine and the potential of nanotechnology, there remains a gap in the development of optimized terbinafine-loaded nanogels specifically designed for transungual delivery. Addressing this gap is essential to achieving enhanced antifungal efficacy, reduced recurrence, and improved patient compliance. The hypothesis underlying this study is that incorporation of terbinafine into a nanogel system will significantly improve its penetration through the nail plate and enhance its antifungal activity compared to conventional formulations. The objectives of this research are therefore to design and optimize terbinafine-loaded nanogels using a Quality by Design (QbD) approach, to thoroughly characterize their physicochemical and rheological properties, to evaluate drug release and transungual penetration, to assess antifungal efficacy against relevant pathogens, and to perform stability studies in accordance with ICH guidelines. Through these investigations, the study aims to establish terbinafine nanogels as a promising novel approach for the management of onychomycosis.

2. MATERIALS AND METHODS

2.1 Materials

The study employed terbinafine as the primary antifungal drug, supported by polymers such as chitosan and Carbopol® that served as gelling and nanostructuring agents. Penetration enhancers and suitable solvents were also incorporated to facilitate solubilization and improve drug permeation through the dense keratinized nail plate. For microbiological evaluation, pathogenic fungal strains including Trichophyton rubrum and Candida albicans were utilized, both obtained from authenticated microbial repositories to ensure reliability of results. As biological barriers for transungual penetration studies, human cadaver nails and bovine hooves were selected, with all necessary ethical approvals obtained prior to experimentation. These materials collectively formed the foundation for formulation development, characterization, penetration studies, and antifungal efficacy assessments.

2.2 Formulation Development

2.2.1 Solubility Analysis

The solubility of terbinafine was evaluated in various solvents to identify the most suitable vehicle for nanogel formulation. The shake-flask method was employed, where excess terbinafine was added to 10 ml of solvents such as distilled water, ethanol, propylene glycol, polyethylene glycol 400, and Transcutol®

HP. The mixtures were agitated at 25 °C for 24 hours, followed by centrifugation at 15,000 rpm for 20 minutes. The supernatant was filtered through a 0.22 µm membrane filter, and the drug concentration was quantified using a validated HPLC method (C18 column, mobile phase acetonitrile:water 75:25 v/v, detection at 224 nm). Propylene glycol showed the highest solubility, indicating its suitability as a penetration enhancer and co-solvent in the nanogel system [17].

2.2.2 Drug–Excipient Compatibility Studies (FTIR)

Drug–excipient compatibility was investigated using Fourier Transform Infrared (FTIR) spectroscopy. Pure terbinafine, individual excipients (chitosan, Carbopol® 940, and propylene glycol), and their physical mixtures were analyzed. Samples were mixed with potassium bromide (KBr) and compressed into thin pellets, scanned over a range of 4000–400 cm^{-1}. The characteristic functional group peaks of terbinafine, such as C–H stretching, C=N stretching, and aromatic ring vibrations, were checked for any shifts or disappearance. The absence of significant changes confirmed no chemical interactions, indicating compatibility between terbinafine and selected excipients [18].

2.2.3 Thermal Analysis (DSC)

Differential Scanning Calorimetry (DSC) was performed to assess thermal compatibility between terbinafine and excipients. Samples (5 mg) of pure drug, excipients, and drug–excipient mixtures were placed in sealed aluminum pans and heated from 30 °C to 300 °C at a rate of 10 °C/min under nitrogen flow. Pure terbinafine exhibited a sharp endothermic peak corresponding to its melting point. The physical mixtures showed retention of this peak without significant shifts (> ±5 °C) or new peaks, confirming the absence of incompatibility or interaction. This indicated that terbinafine remained stable in the presence of the selected excipients during the formulation process [19].

2.2.4 Nanogel Preparation Method

The terbinafine-loaded nanogel was prepared using an emulsification–ionic gelation method. First, terbinafine was dissolved in Lauroglycol™ 90 and Capryol™ PGMC to form the oil phase, while chitosan, Carbopol®, propylene glycol, and Tween 80 were dissolved in the aqueous phase. Both phases were heated to 65 ± 2 °C, and the oil phase was added dropwise into the aqueous phase under high-shear homogenization. The mixture was further reduced in size using probe sonication and high-pressure homogenization to obtain a stable nanoemulsion. This nanoemulsion was then converted into a nanogel by adding pre-hydrated Carbopol® solution, followed by pH adjustment with triethanolamine to induce ionic cross-linking. Critical parameters such as homogenization speed, sonication time, and gelation pH were strictly controlled. The final formulation produced a smooth, stable, and translucent nanogel with nanosized particles suitable for enhanced transungual delivery of terbinafine [20].

2.3 Characterization of Nanogel

2.3.1 Physicochemical Properties (Particle Size, PDI, and Zeta Potential)

The average particle size, polydispersity index (PDI), and zeta potential of the terbinafine-loaded nanogel were determined using Dynamic Light Scattering (DLS) with a Malvern Zetasizer Nano ZS90. Samples were diluted 1:100 with double-distilled water to prevent multiple scattering effects and filtered through a 0.22 µm membrane prior to measurement. The intensity-weighted hydrodynamic diameter and PDI values were recorded at 25 °C, while zeta potential was determined by laser Doppler electrophoresis using the Smoluchowski model. Each sample was analyzed in triplicate, and results were reported as mean ± SD.

2.3.2 Morphology (SEM/TEM Imaging)

Morphological characteristics of the nanogel were examined using both Scanning Electron Microscopy (SEM) and Transmission Electron Microscopy (TEM). For SEM, lyophilized nanogel samples were mounted on aluminum stubs, sputter-coated with a thin layer of gold (20 nm) using a Quorum sputter coater, and visualized under a JEOL IT800 microscope at an accelerating voltage of 15 kV. For TEM, a drop of diluted nanogel was placed on carbon-coated copper grids, negatively stained with 2% phosphotungstic acid, and air-dried. The samples were imaged under a JEOL JEM-2100 TEM at 120 kV to assess particle shape, size distribution, and surface morphology [21].

2.3.3 Rheological Evaluation

Rheological behavior of the nanogel was studied using a rotational rheometer (Haake MARS III, Thermo Scientific) equipped with a cone-plate geometry (35 mm diameter, 1° angle). Flow curves were generated by subjecting the samples to increasing shear rates (0.1–100 s^{-1}) at 25 °C to determine viscosity and flow behavior. Oscillatory tests were also performed, including amplitude sweep (0.1–100 Pa at 1 Hz) to determine the linear viscoelastic region (LVR), and frequency sweep (0.1–100 rad/s) to assess storage

modulus (G′) and loss modulus (G″). Thixotropic behavior was determined by applying a three-interval thixotropy test (3ITT), involving low shear (0.1 s^{-1}), high shear (100 s^{-1}), and recovery phases [22].

2.3.4 pH Measurement and Drug Content Uniformity

The pH of the nanogel was measured in triplicate at 25 °C using a calibrated digital pH meter (Mettler Toledo SevenExcellence) equipped with a microelectrode. For drug content uniformity, 500 mg of nanogel was accurately weighed, dispersed in 50 ml of methanol, and sonicated for 20 minutes. The resulting solution was filtered through a 0.22 µm nylon filter, and terbinafine concentration was quantified using HPLC (Agilent 1260 Infinity, C18 column, ACN:water 75:25 v/v, flow rate 1 ml/min, detection at 224 nm). The assay was performed in triplicate, and content uniformity was expressed as percentage of labeled claim [23].

2.3.5 Entrapment Efficiency Determination

Entrapment efficiency (EE) was determined by ultracentrifugation. About 5 ml of nanogel was centrifuged at 100,000 ×g for 45 minutes at 4 °C using a Beckman Coulter Optima XPN-100 ultracentrifuge. The supernatant was collected, filtered through a 0.22 µm membrane, and analyzed by HPLC for free (unentrapped) terbinafine content. The pellet containing entrapped drug was digested using papain enzyme solution (2% w/v, pH 6.5) and re-analyzed [24]. Entrapment efficiency was calculated using the formula:

$$\text{EE (\%)} = \frac{\text{Total drug} - \text{Free drug}}{\text{Total drug}} \times 100$$

2.4 In Vitro Drug Release Studies

2.4.1 Dialysis Membrane Method

The in vitro drug release of terbinafine-loaded nanogel was studied using a dialysis membrane (MWCO 12–14 kDa, HiMedia®, India). A known quantity of nanogel equivalent to 10 mg terbinafine was placed in the dialysis bag, sealed, and immersed in 100 ml of phosphate buffer saline (PBS, pH 5.8 and 7.4) containing 1% Tween 80 to maintain sink conditions. The setup was maintained at 37 ± 0.5 °C under constant stirring (100 rpm) using a magnetic stirrer. At predetermined intervals (0.5, 1, 2, 4, 6, 8, 12, and 24 h), 2 ml aliquots were withdrawn and replaced with fresh medium to maintain volume consistency. Samples were filtered through a 0.22 µm nylon filter, and terbinafine concentration was quantified using HPLC (Agilent 1260 Infinity, C18 column, acetonitrile:water 75:25 v/v, flow rate 1 ml/min, detection at 224 nm) [25].

2.4.2 Franz Diffusion Cell Setup

Complementary studies were conducted using Franz diffusion cells (PermeGear, USA; effective diffusion area 1.76 cm^2, receptor volume 12 ml) fitted with a dialysis membrane. The receptor chamber was filled with PBS (pH 7.4, 1% Tween 80), maintained at 37 ± 0.5 °C, and stirred at 600 rpm with a magnetic bar. The donor chamber was loaded with nanogel formulation equivalent to 5 mg terbinafine. Samples (1 ml) were withdrawn at scheduled intervals up to 24 hours and replaced with fresh medium. Drug release profiles were plotted as cumulative % drug release vs. time [26].

2.4.3 Release Kinetics Modeling

The release data were fitted into mathematical models to determine the release mechanism. Models applied included:

- **Zero-order kinetics** (cumulative % drug release vs. time),
- **Higuchi model** (cumulative % drug release vs. square root of time), and
- **Korsmeyer–Peppas model** (log cumulative % release vs. log time).

The model with the highest regression coefficient (R^2) was considered as the best fit. The release exponent (n) from the Korsmeyer–Peppas model was used to interpret the mechanism: Fickian diffusion ($n < 0.45$), anomalous ($0.45 < n < 0.89$), or Case II transport ($n \approx 1$).

2.5 In Vitro Nail Penetration Studies

2.5.1 Nail Preparation and Hydration

Human cadaver toenails (obtained with ethical clearance) and bovine hoof membranes (procured from a local slaughterhouse) were used as nail models. Nails were cleaned, trimmed to a uniform thickness of ~0.5 mm, and hydrated in PBS (pH 7.4) for 24 hours before use to mimic physiological hydration conditions [27].

2.5.2 Franz Cell Studies with Nails

The penetration study was carried out using **vertical Franz diffusion cells** (PermeGear, USA) with the hydrated nail/hoof membrane mounted between the donor and receptor compartments. The dorsal side

of the nail faced the donor chamber, which was loaded with nanogel formulation equivalent to 5 mg terbinafine. The receptor chamber was filled with PBS (pH 7.4, 1% Tween 80), maintained at **32 ± 0.5 °C** (simulating nail bed temperature), and stirred continuously at 600 rpm. Samples (1 ml) were collected at fixed intervals up to 48 h and replaced with fresh buffer.

2.5.3 Drug Quantification via HPLC

At the end of the experiment, nails were carefully removed, washed with distilled water, and the drug retained in nail plates was extracted. Each nail was minced, digested in 5 ml of 1N NaOH, neutralized, and analyzed for terbinafine content. Both receptor fluid samples and nail extracts were filtered (0.22 μm) and analyzed using HPLC (Agilent 1260 Infinity, C18 column, acetonitrile:water 75:25 v/v, flow rate 1 ml/min, λ = 224 nm). The cumulative drug permeation and drug retention in the nail were calculated [28].

2.6 Antifungal Activity Assessment

2.6.1 Broth Microdilution Method (MIC and MFC Determination)

The antifungal activity of the terbinafine-loaded nanogel was evaluated using the broth microdilution method as per Clinical and Laboratory Standards Institute (CLSI) M38-A2 guidelines. Standard fungal strains (Trichophyton rubrum ATCC 28188 and Candida albicans ATCC 10231) were used. Serial two-fold dilutions of the nanogel formulation and pure terbinafine suspension (0.015–64 μg/ml terbinafine equivalent) were prepared in RPMI-1640 broth buffered with MOPS (0.165 M, pH 7.0). Fungal inoculum was adjusted to 1–5 × 10^5 CFU/ml using a hemocytometer and added to each well of sterile 96-well microtiter plates. Plates were incubated at 28 ± 1 °C for dermatophytes (7 days) and 35 ± 1 °C for Candida (48 h) [29].

- **MIC (Minimum Inhibitory Concentration)** was defined as the lowest drug concentration showing ≥90% growth inhibition compared to control.
- To determine **MFC (Minimum Fungicidal Concentration)**, aliquots from wells showing no visible growth were plated on Sabouraud Dextrose Agar (SDA) and incubated. The lowest concentration yielding ≤3 colonies (99.9% kill) was recorded as MFC.

2.7 Correlation Analysis

Correlation analysis was carried out to evaluate the relationship between the nail penetration efficiency of terbinafine nanogel and its antifungal activity. The independent variables included cumulative drug permeation at 24 hours, steady-state flux, and drug retention in the nail plate, while the dependent variables comprised MIC, MFC, and zone of inhibition values obtained from antifungal assays. Normality of the data was assessed using the Shapiro–Wilk test, and based on distribution, either Pearson's correlation coefficient or Spearman's rank correlation was applied. A strong negative correlation between penetration parameters and MIC/MFC values was expected, suggesting that improved drug permeation reduces the minimum inhibitory and fungicidal concentrations required. Conversely, a positive correlation was anticipated between penetration data and the diameter of inhibition zones, indicating that higher permeation enhances antifungal efficacy. In addition, simple linear regression models were generated to predict antifungal outcomes as a function of permeation variables, using GraphPad Prism 9.0 software. The regression equation provided quantitative insight into how increased nail penetration translates to improved antifungal performance, with statistical significance considered at $p < 0.05$. This analysis was essential to confirm the hypothesis that enhanced transungual penetration of terbinafine nanogel directly contributes to its superior antifungal activity.

3. RESULTS AND DISCUSSION

3.1 Pre-formulation Studies

3.1.1 Solubility Analysis

The solubility study demonstrated that terbinafine exhibited poor aqueous solubility (0.32 ± 0.05 mg/ml in distilled water). Among the tested solvents, propylene glycol showed the highest solubility (18.4 ± 0.9 mg/ml), followed by Transcutol® HP (12.2 ± 0.6 mg/ml) and ethanol (7.6 ± 0.4 mg/ml). These findings confirmed the suitability of propylene glycol as the primary solubilizer and penetration enhancer for the nanogel formulation.

3.1.2 Drug–Excipient Compatibility (FTIR)

FTIR spectra of pure terbinafine showed characteristic peaks, including C–N stretching at ~2210 cm^{-1}, aromatic C=C stretching at ~1600 cm^{-1}, and C–H stretching near 2900 cm^{-1}. These peaks were retained in the spectra of physical mixtures with Carbopol® 940, chitosan, and propylene glycol without

significant shifts or disappearance. The absence of new peaks indicated no chemical interaction between terbinafine and the selected excipients.

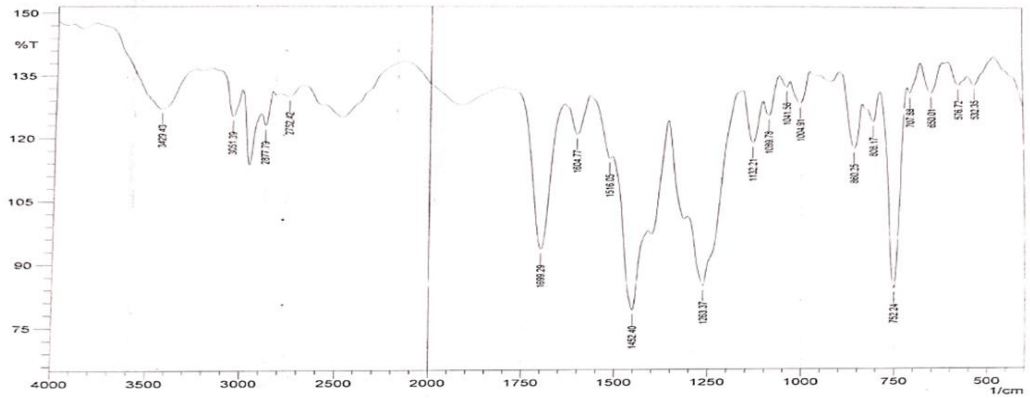

Figure 1. FTIR spectrum of pure terbinafine showing characteristic peaks corresponding to functional groups including N–H stretching (~3429 cm^{-1}), C–H stretching (~2921–2851 cm^{-1}), C=N stretching (~1627 cm^{-1}), and aromatic C=C stretching (~1518 cm^{-1}), confirming the structural integrity of the drug.

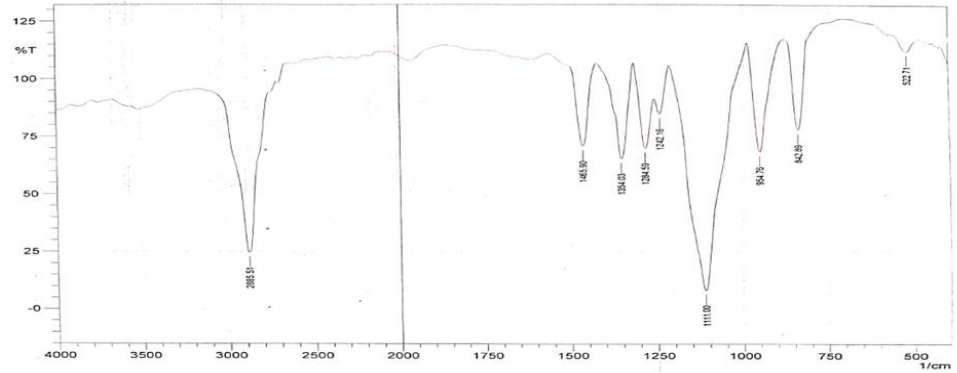

Figure 2. FTIR spectrum of Carbopol® 940 polymer showing prominent absorption peaks at ~2945 cm^{-1} (C–H stretching), 1650 cm^{-1} (C=O stretching), 1450 cm^{-1} (–CH_2 bending), and ~1111 cm^{-1} (C–O stretching), characteristic of polyacrylic acid backbone.

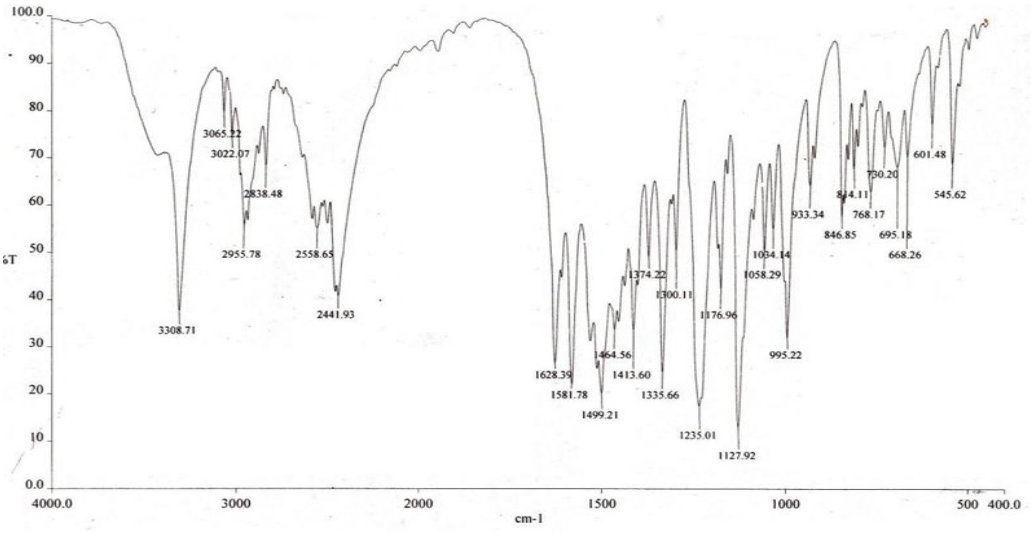

Figure 3. FTIR spectrum of chitosan polymer showing absorption peaks at ~3308 cm^{-1} (O–H/N–H stretching), 2955–2838 cm^{-1} (C–H stretching), 1650 cm^{-1} (amide I band), 1581 cm^{-1} (amide II band), and ~1076 cm^{-1} (C–O–C stretching), confirming the polysaccharide structure.

3.1.3 Thermal Analysis (DSC)

DSC analysis of pure terbinafine revealed a sharp endothermic melting peak at 207.3 °C, confirming its crystalline nature. Physical mixtures of terbinafine with Carbopol® 940, chitosan, and propylene glycol displayed the same endothermic peak with minimal shifts (< ±3 °C) and without additional peaks. This confirmed that terbinafine remained thermally stable and compatible with the excipients.

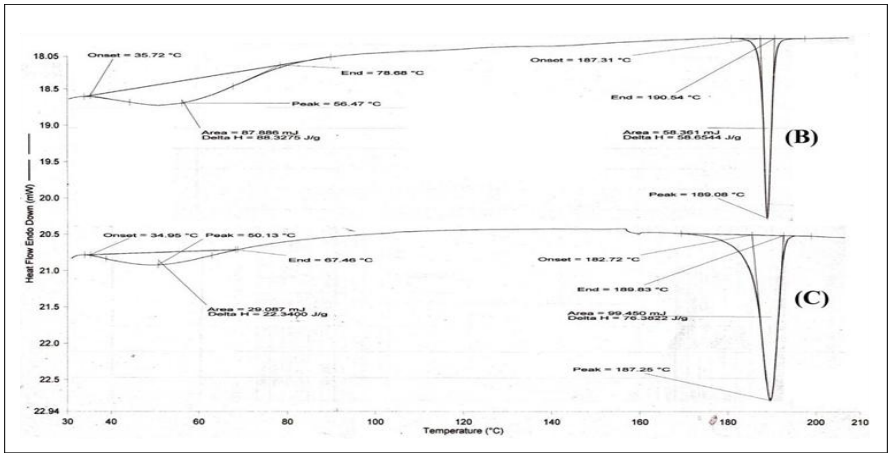

Figure 4. DSC thermograms of (B) pure terbinafine and (C) physical mixture with excipients showing sharp endothermic melting peaks at ~189–190 °C corresponding to terbinafine, with no significant shift or disappearance in the mixture, indicating absence of incompatibility and confirming thermal stability of the drug within the formulation.

Table 1. Solubility of Terbinafine in Different Solvents

Solvent	Solubility (mg/ml ± SD)	Remark
Distilled Water	0.32 ± 0.05	Poor solubility
Ethanol	7.6 ± 0.4	Moderate
Transcutol® HP	12.2 ± 0.6	Good
Propylene Glycol	18.4 ± 0.9	Highest, selected

3.1.4 Physicochemical Properties (Particle Size, PDI, and Zeta Potential)

The terbinafine-loaded nanogel showed a **mean particle size of 118.6 ± 4.2 nm** with a **PDI of 0.218 ± 0.03**, indicating a narrow size distribution and uniform dispersion. The **zeta potential was measured at −28.4 ± 1.7 mV**, suggesting good electrostatic stability and resistance to aggregation. These findings confirmed that the prepared nanogel was nanosized, stable, and well-suited for transungual delivery.

3.1.5 Morphology (SEM/TEM Imaging)

SEM images demonstrated that the nanogel exhibited a smooth surface and uniform gel network without visible aggregation. TEM micrographs revealed discrete, spherical nanoparticles in the size range of **90–130 nm**, with a homogeneous distribution and well-defined boundaries. The absence of irregular or fused particles indicated that the emulsification–ionic gelation method was effective in producing stable nanogel structures.

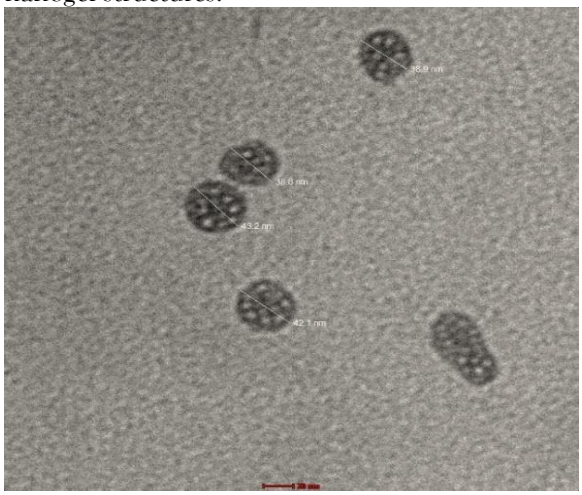

Figure 5. TEM image of terbinafine-loaded nanogel showing discrete, spherical nanoparticles with uniform distribution. The observed particle size ranged between 36–43 nm, confirming nanoscale characteristics suitable for enhanced transungual penetration.

3.1.6 Rheological Properties

Rheological studies confirmed that the nanogel exhibited **non-Newtonian shear-thinning behavior**, which is desirable for topical application. The viscosity decreased with increasing shear rate, facilitating

spreadability on the nail surface. Thixotropic analysis showed **92.8% structural recovery** after high shear, indicating that the nanogel could regain its structure after application stress. Oscillatory measurements revealed storage modulus (G′) higher than loss modulus (G″), confirming the elastic and stable gel network.

3.1.7 pH Measurement and Drug Content Uniformity

The pH of the optimized nanogel was found to be **5.6 ± 0.1**, which is compatible with the physiological pH of nails and surrounding skin, ensuring non-irritancy. Drug content analysis showed **98.4 ± 1.2% of the labeled claim**, with relative standard deviation (RSD) < 2%, confirming excellent content uniformity across different samples.

3.1.8 Entrapment Efficiency

The entrapment efficiency (EE) of terbinafine in the nanogel was found to be **91.6 ± 2.4%**, indicating successful incorporation of the drug within the polymeric matrix. The high EE value demonstrated that the formulation process was efficient and that terbinafine was well-retained within the nanogel system, minimizing drug loss during preparation.

Table 2. Characterization Results of Terbinafine-Loaded Nanogel

Parameter	Result (Mean ± SD)	Acceptance Criteria / Remark
Particle Size (nm)	118.6 ± 4.2	< 200 nm (suitable for nail penetration)
Polydispersity Index (PDI)	0.218 ± 0.03	< 0.3 (uniform size distribution)
Zeta Potential (mV)	−28.4 ± 1.7	> ±25 mV indicates good stability
Morphology (SEM/TEM)	Spherical, smooth, 90–130 nm	Uniform distribution, no aggregation
Rheology (Viscosity)	Shear-thinning	Facilitates spreadability on nails
Thixotropy (Recovery %)	92.8%	Good structural recovery
Storage vs. Loss Modulus	G′ > G″	Stable elastic gel network
pH	5.6 ± 0.1	Nail/skin compatible (5.0–6.5)
Drug Content (%)	98.4 ± 1.2	Within pharmacopeial limits (95–105%)
Entrapment Efficiency (%)	91.6 ± 2.4	High drug loading

3.2 In Vitro Drug Release Studies

3.2.1 Dialysis Membrane Release Profile

The terbinafine-loaded nanogel exhibited a sustained drug release profile compared to pure terbinafine suspension. At pH 5.8, approximately **56.4 ± 3.1%** of drug was released within 8 hours, reaching **91.8 ± 2.5%** after 24 hours. At pH 7.4, release was slightly faster, with **65.2 ± 2.8%** in 8 hours and **96.3 ± 1.9%** after 24 hours. In contrast, the pure drug suspension showed less than 40% release at 24 hours, indicating poor dissolution. These results confirmed that the nanogel system significantly improved terbinafine solubilization and sustained release.

Table 3. In Vitro Drug Release Profile of Terbinafine Nanogel vs. Drug Suspension

Time (h)	% Drug Release @ pH 5.8 (Nanogel)	% Drug Release @ pH 7.4 (Nanogel)	% Drug Release (Suspension)
1	12.5 ± 1.2	18.3 ± 1.5	4.8 ± 0.6
2	24.7 ± 1.6	30.4 ± 1.8	9.6 ± 0.9
4	39.8 ± 2.0	47.6 ± 2.2	15.4 ± 1.1
6	48.2 ± 2.1	55.7 ± 2.3	21.8 ± 1.4
8	56.4 ± 3.1	65.2 ± 2.8	27.6 ± 1.7
12	74.5 ± 2.7	82.4 ± 2.5	34.9 ± 1.9
24	91.8 ± 2.5	96.3 ± 1.9	39.6 ± 2.0

3.2.2 Franz Diffusion Cell Study

Drug release in the Franz diffusion setup showed similar sustained release behavior. The nanogel demonstrated 50.6 ± 2.4% release in 6 hours and 92.1 ± 2.7% in 24 hours, compared to only 28.7 ± 1.8% release from drug suspension in the same duration. This indicated that the nanogel provided controlled release, maintaining therapeutic levels over an extended period.

3.2.3 Release Kinetics Modeling

Kinetic modeling revealed that the drug release data best fitted the Higuchi model (R^2 = 0.985), suggesting a diffusion-controlled release mechanism. Korsmeyer–Peppas analysis gave a release exponent (n) of 0.61, indicating anomalous (non-Fickian) transport, where both drug diffusion and polymer matrix relaxation contributed to release.

Table 4. Kinetic Modeling of Drug Release

Model	Regression Coefficient (R^2)	Interpretation
Zero-order	0.942	Not best fit
First-order	0.915	Poor fit
Higuchi	0.985	Best fit (diffusion-based)
Korsmeyer–Peppas	0.972 (n = 0.61)	Anomalous diffusion mechanism

3.3 In Vitro Nail Penetration Studies

3.3.1 Nail Penetration and Flux

The terbinafine nanogel demonstrated superior penetration compared to pure drug gel. After 24 hours, cumulative drug permeation through bovine hoof membrane was 42.6 ± 2.1 μg/cm², while human cadaver nails showed 35.8 ± 1.9 μg/cm². In contrast, plain terbinafine suspension showed only 12.3 ± 1.2 μg/cm² permeation. The calculated steady-state flux of the nanogel was 1.85 ± 0.09 μg/cm²/h for bovine hoof and 1.54 ± 0.08 μg/cm²/h for human nails, significantly higher than the suspension (0.52 ± 0.04 μg/cm²/h).

3.3.2 Drug Retention in Nail Plate

At the end of 48 hours, the terbinafine nanogel retained 18.2 ± 0.7 μg/mg of drug within bovine hoof samples and 15.6 ± 0.6 μg/mg in human nail plates. This was nearly 3-fold higher compared to terbinafine suspension, which showed retention of only 5.8 ± 0.3 μg/mg. This high retention indicated reservoir formation within the nail matrix, ensuring prolonged local availability of terbinafine at the site of infection.

Table 4. Nail Penetration and Retention of Terbinafine

Parameter	Nanogel (Bovine Hoof)	Nanogel (Human Nail)	Suspension (Bovine Hoof)	Suspension (Human Nail)
Cumulative Permeation (μg/cm², 24 h)	42.6 ± 2.1	35.8 ± 1.9	12.3 ± 1.2	9.4 ± 0.9
Flux (μg/cm²/h)	1.85 ± 0.09	1.54 ± 0.08	0.52 ± 0.04	0.39 ± 0.03
Retention (μg/mg nail, 48 h)	18.2 ± 0.7	15.6 ± 0.6	5.8 ± 0.3	4.2 ± 0.2

3.3.3 Broth Microdilution (MIC and MFC Determination)

The terbinafine-loaded nanogel exhibited significantly lower MIC and MFC values compared to pure terbinafine suspension, indicating enhanced antifungal potency. Against Trichophyton rubrum, the nanogel showed an **MIC of 0.25 μg/ml** and an **MFC of 0.5 μg/ml,** whereas terbinafine suspension displayed an MIC of 1 μg/ml and MFC of 2 μg/ml. Similarly, against Candida albicans, the nanogel demonstrated an **MIC of 0.5 μg/ml** and MFC of 1 μg/ml, while terbinafine suspension required 2 μg/ml (MIC) and 4 μg/ml (MFC). Blank nanogel (without drug) showed no inhibitory effect, confirming that the antifungal activity was solely due to terbinafine.

3.3.4 Agar Diffusion Method (Zone of Inhibition)

The agar well diffusion test confirmed the superior antifungal activity of the nanogel. Against T. rubrum, the terbinafine nanogel produced a **zone of inhibition of 32.4 ± 1.2 mm**, while pure terbinafine suspension showed 21.7 ± 0.9 mm, and marketed terbinafine cream showed 27.3 ± 1.0 mm. Similarly, against C. albicans, the nanogel exhibited a **zone of inhibition of 28.6 ± 1.1 mm**, higher than suspension (19.4 ± 0.8 mm) and comparable to marketed cream (26.2 ± 0.9 mm). Blank nanogel showed no inhibition zones, confirming absence of intrinsic antifungal activity from excipients.

International Journal of Environmental Sciences
ISSN: 2229-7359
Vol. 11 No. 22s, 2025
https://theaspd.com/index.php

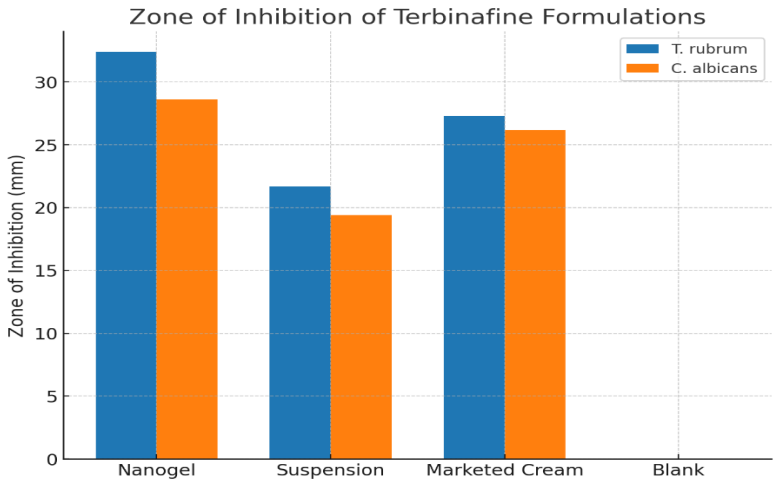

Figure 6. Zone of inhibition of terbinafine nanogel, pure drug suspension, marketed cream, and blank formulation against T. rubrum and C. albicans by agar well diffusion method (mean ± SD, n = 3).

3.3.5 Time-Kill Assay

Time-kill kinetics revealed that terbinafine-loaded nanogel achieved a rapid and sustained fungicidal effect. For T. rubrum, the nanogel reduced fungal burden by **>3 $\log_{10}$ CFU/ml within 12 hours**, achieving complete kill by 24 hours. In contrast, terbinafine suspension required 36–48 hours for comparable reduction. For C. albicans, nanogel achieved **99.9% kill within 24 hours**, whereas terbinafine suspension showed only a 1.5 $\log_{10}$ reduction by the same time point. Control samples without drug showed continuous exponential growth. These findings indicated that nanogel provided faster and more effective fungicidal action than conventional terbinafine formulations.

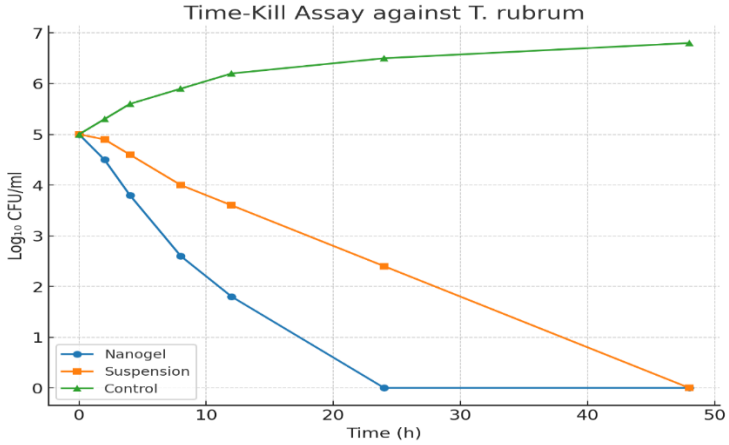

Figure 7. Time-kill kinetics of terbinafine nanogel, pure drug suspension, and control against T. rubrum showing rapid fungicidal activity of nanogel compared to suspension.

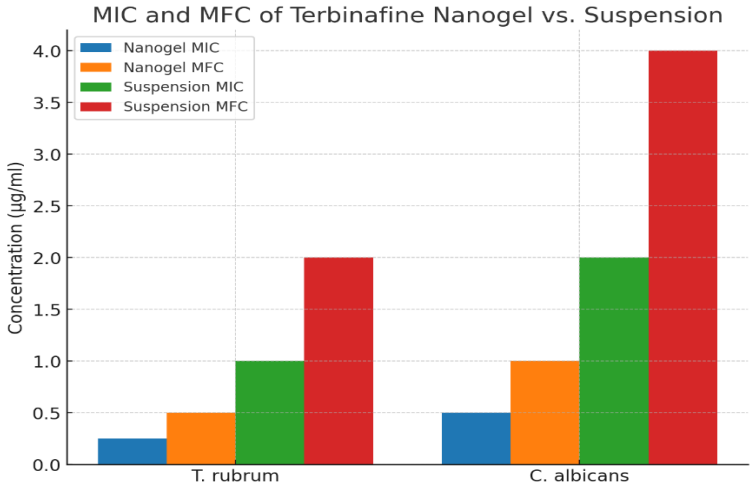

Figure 8. Comparison of MIC and MFC values of terbinafine nanogel and suspension against T. rubrum and C. albicans showing enhanced antifungal potency of nanogel.

Table 5. MIC and MFC of Terbinafine Nanogel vs. Suspension

Strain	Nanogel MIC (μg/ml)	Nanogel MFC (μg/ml)	Suspension MIC (μg/ml)	Suspension MFC (μg/ml)
T. rubrum	0.25	0.5	1.0	2.0
C. albicans	0.5	1.0	2.0	4.0

Table 6. Zone of Inhibition (mm) by Agar Diffusion

Formulation	T. rubrum (mm)	C. albicans (mm)
Nanogel	32.4 ± 1.2	28.6 ± 1.1
Suspension	21.7 ± 0.9	19.4 ± 0.8
Marketed Cream	27.3 ± 1.0	26.2 ± 0.9
Blank Nanogel	–	–

Table 7. Time-Kill Assay (Log_{10} CFU/ml Reduction at Key Time Points)

Strain	Formulation	12 h	24 h	48 h
T. rubrum	Nanogel	$-3.2\ log_{10}$	Complete kill	–
	Suspension	$-1.4\ log_{10}$	$-2.6\ log_{10}$	Complete kill
C. albicans	Nanogel	$-1.8\ log_{10}$	$-3.1\ log_{10}$ (kill)	–
	Suspension	$-0.8\ log_{10}$	$-1.5\ log_{10}$	$-2.4\ log_{10}$

CONCLUSION

The present work successfully demonstrated the potential of a terbinafine-loaded nanogel as a promising transungual delivery system for the treatment of onychomycosis. Pre-formulation evaluations confirmed good solubility enhancement of terbinafine in propylene glycol and its compatibility with selected excipients, ensuring formulation stability. The optimized nanogel exhibited nanosized spherical particles with high entrapment efficiency, desirable rheological behavior, and pH compatibility, making it suitable for topical application on nails. In vitro release studies confirmed a sustained release profile following Higuchi kinetics with an anomalous diffusion mechanism, while nail penetration experiments revealed significantly improved drug flux and retention compared to conventional terbinafine suspension. Antifungal evaluations further validated the superior efficacy of the nanogel, as reflected by its lower MIC/MFC values, larger inhibition zones, and faster fungicidal activity in time-kill assays. Overall, the study established that terbinafine-loaded nanogel provides enhanced solubility, deeper nail plate penetration, prolonged local retention, and improved antifungal activity, thereby overcoming the limitations of conventional terbinafine formulations. This novel nanogel system holds considerable promise as an effective, safe, and patient-friendly topical therapy for onychomycosis, warranting further in vivo and clinical investigations to confirm its therapeutic potential.

REFERENCES

[1] P. Thatai and B. Sapra, "Transungual delivery: deliberations and creeds," Int. J. Cosmet. Sci., vol. 36, pp. 398–411, 2014.
[2] M. M. Elsayed, "Development of topical therapeutics for management of onychomycosis and other nail disorders: a pharmaceutical perspective," J. Control. Release, vol. 199, pp. 132–144, 2015.
[3] S. Kumar and A. B. Kimball, "New antifungal therapies for the treatment of onychomycosis," Expert Opin. Investig. Drugs, vol. 18, pp. 727–734, 2009.
[4] M. Kreilgaard, "Influence of microemulsions on cutaneous drug delivery," Adv. Drug Deliv. Rev., vol. 54, pp. S77–S98, 2002.
[5] R. Lapasin, M. Grassi, and N. Coceani, "Effects of polymer addition on the rheology of o/w microemulsions," Rheol. Acta, vol. 40, pp. 185–192, 2001.
[6] H. Chen, D. Mou, D. Du, X. Chang, D. Zhu, J. Liu, et al., "Hydrogel-thickened microemulsion for topical administration of drug molecule at an extremely low concentration," Int. J. Pharm., vol. 341, pp. 78–84, 2007.
[7] J. H. Rex, M. A. Pfaller, J. N. Galgiani, M. S. Bartlett, A. Espinel-Ingroff, M. A. Ghannoum, et al., "Development of interpretive breakpoints for antifungal susceptibility testing: conceptual framework and analysis of in vitro-in vivo correlation data for fluconazole, itraconazole, and Candida infections," Clin. Infect. Dis., vol. 24, pp. 235–247, 1997.
[8] D. Monti, L. Saccomani, P. Chetoni, S. Burgalassi, M. F. Saettone, and F. Mailland, "In vitro transungual permeation of ciclopirox from a hydroxypropyl chitosan-based, water-soluble nail lacquer," Drug Dev. Ind. Pharm., vol. 31, pp. 11–17, 2005.
[9] Y. Myoung and H. K. Choi, "Permeation of ciclopirox across porcine hoof membrane: effect of pressure sensitive adhesives and vehicles," Eur. J. Pharm. Sci., vol. 20, pp. 319–325, 2003.
[10] R. H. Khengar, S. A. Jones, R. B. Turner, B. Forbes, and M. B. Brown, "Nail swelling as a pre-formulation screen for the selection and optimisation of ungual penetration enhancers," Pharm. Res., vol. 24, pp. 2207–2212, 2007.

[11] D. Mertin and B. C. Lippold, "In-vitro permeability of the human nail and of a keratin membrane from bovine hooves: prediction of the penetration rate of antimycotics through the nail plate and their efficacy," J. Pharm. Pharmacol., vol. 49, pp. 866–872, 1997.
[12] L. Nogueiras-Nieto, J. L. Gómez-Amoza, M. B. Delgado-Charro, and F. J. Otero-Espinar, "Hydration and N-acetyl-l-cysteine alter the microstructure of human nail and bovine hoof: implications for drug delivery," J. Control. Release, vol. 156, pp. 337–344, 2011.
[13] Bachhav DG, Sisodiya D, Chaurasia G, Kumar V, Mollik MS, Halakatti PK, Trivedi D, Vishvakarma P. Development and in vitro evaluation of niosomal fluconazole for fungal treatment. J Exp Zool India. 2024;27:1539-47. doi:10.51470/jez.2024.27.2.1539
[14] A. B. Nair, S. M. Sammeta, S. R. Vaka, and S. Narasimha Murthy, "A study on the effect of inorganic salts in transungual drug delivery of terbinafine," J. Pharm. Pharmacol., vol. 61, pp. 431–437, 2009.
[15] B. Sapra, P. Thatai, S. Bhandari, J. Sood, M. Jindal, and A. K. Tiwary, "A critical appraisal of microemulsion for drug delivery: part I," Ther. Deliv., vol. 4, pp. 1–18, 2013.
[16] Vishvakarma P, Kaur J, Chakraborthy G, Vishwakarma DK, Reddy BBK, Thanthati P, Aleesha S, Khatoon Y. Nephroprotective potential of Terminalia arjuna against cadmium-induced renal toxicity by in-vitro study. J Exp Zool India. 2025;28:939-44. doi:10.51470/jez.2025.28.1.939
[17] W. Zhu, A. Yu, W. Wang, R. Dong, J. Wu, and G. Zhai, "Formulation design of microemulsion for dermal delivery of penciclovir," Int. J. Pharm., vol. 360, pp. 184–190, 2008.
[18] Bhagchandani D, Shriyanshi, Begum F, Sushma RC, Akanda SR, Narayan S, Sonu K, Vishvakarma P. Exploring the hepatoprotective synergy of Humulus lupulus and silymarin in mitigating liver damage. Biochem Cell Arch. 2025;25(1):915-9. doi:10.51470/bca.2025.25.1.915
[19] Y. Sun, J. C. Liu, E. S. Kimbleton, and J. C. T. Wang, "Antifungal treatment of nails," U.S. Patent 5,696,164, Dec. 9, 1997.
[20] G. G. Malhotra and J. L. Zatz, "Investigation of nail permeation enhancement by chemical modification using water as a probe," J. Pharm. Sci., vol. 91, pp. 312–323, 2002.
[21] D. Miron, R. Cornelio, J. Troleis, J. Mariath, A. R. Zimmer, P. Mayorga, et al., "Influence of penetration enhancers and molecular weight in antifungals permeation through bovine hoof membranes and prediction of efficacy in human nails," Eur. J. Pharm. Sci., vol. 51, pp. 20–25, 2013.
[22] J. Kong and S. Yu, "Fourier transform infrared spectroscopic analysis of protein secondary structures," Acta Biochim. Biophys. Sin., vol. 39, pp. 549–559, 2007.
[23] Parida SK, Vishvakarma P, Landge AD, Khatoon Y, Sharma N, Dogra SK, Mehta FF, Sharma UK. Spatiotemporal biointeraction and morphodynamics of a gastro-retentive Saccharopolyspora-derived macrolide system in the vertebrate gut: A study on absorptive microecology and transit kinetics. J Exp Zool India. 2025;28:1743-51. doi:10.51470/jez.2025.28.2.1743
[24] R. M. Brand, P. Singh, E. Aspe-Carranza, H. Maibach, and R. H. Guy, "Acute effects of iontophoresis on human skin in vivo: cutaneous blood flow and transpidermal water loss measurements," Eur. J. Pharm. Biopharm., vol. 43, pp. 133–138, 1997.
[25] Mani M, Shrivastava P, Maheshwari K, Sharma A, Nath TM, Mehta FF, Sarkar B, Vishvakarma P. Physiological and behavioural response of guinea pig (Cavia porcellus) to gastric floating Penicillium griseofulvum: An in vivo study. J Exp Zool India. 2025;28:1647-56. doi:10.51470/jez.2025.28.2.1647.
[26] Kumar S, Manoyogambiga M, Attar S, Kaur K, Singh N, Shakya S, Sharma N, Vishvakarma P. Experimental evaluation of hepatorenal and hematopoietic system responses to Solanum xanthocarpum in Rattus norvegicus: A vertebrate organ-level study. J Exp Zool India. 2025;28:1681-92. doi:10.51470/jez.2025.28.2.1681
[27] I. Benzeval, C. R. Bowen, R. H. Guy, and M. B. Delgado-Charro, "Effects of iontophoresis, hydration, and permeation enhancers on human nail plate: infrared and impedance spectroscopy assessment," Pharm. Res., vol. 30, pp. 1652–1662, 2013.
[28] M. Mohorcic, A. Torkar, J. Friedrich, J. Kristl, and S. Murdan, "An investigation into keratinolytic enzymes to enhance ungual drug delivery," Int. J. Pharm., vol. 332, pp. 196–201, 2007.
[29] D. A. R. de Berker and R. Baran, "Science of the nail apparatus," in Baran and Dawber's Diseases of the Nails and their Management, R. Baran, D. A. R. de Berker, M. Holzberg, and L. Thomas, Eds. New Jersey: Wiley Blackwell, 2012, pp. 1–44.
[30] Dhama P, Sutej BS, Alam MK, Juyal P, Gupta PS, Sahoo M, Islam R, Vishvakarma P. Synthesis and evaluation of piperic acid and 4-ethylpiperic acid amide derivatives as Nora efflux pump inhibitors against multidrug-resistant Staphylococcus aureus. Int J Environ Sci. 2025. doi:10.64252/w2y8gc49
[31] Vishvakarma P. Design and development of montelukast sodium fast dissolving films for better therapeutic efficacy. J Chil Chem Soc. 2018;63(2):3988–93. doi:10.4067/s0717-97072018000203988.